DOI 10.4467/21995923GP.23.002.18601 GEOINFORMATICA POLONICA
22: 2023

Tomisław Gołębiowski[1]
ORCID: 0000-0002-4005-2265

GPR SIGNAL ANALYSIS FOR THE EXPLORATION OF LOOSE ZONES IN THE NEAR SURFACE UNDERGROUND

[1]Cracow University of Technology
Faculty of Environmental Engineering and Energy
Department of Geoengineering and Water Management
tomislaw.golebiowski@pk.edu.pl

Abstract

In the paper, non-standard signal and image processing applied for the GPR (Ground Penetrating Radar) data record for various antennae orientations was presented and discussed. The terrain surveys were carried out in the post-mining region in Poland where numerous sinkholes and subsidence areas were observed on the surface due to the former mining activity. The GPR surveys were conducted between two existing sinkholes and the aim of measurements was detection of loose zones in the ground created by suffosion process which caused the formation of the mentioned two sinkholes. In the paper, the Author proposed a new way of processing and analysis of radargrams based on three steps, i.e. 1D more advanced processing of signals/traces, 2D more advanced image processing of combined radarogram, visualisation and analysis of selected signal attributes.

Keywords: GPR, signal attributes, various orientations of antennae, suffosion, post-mining region

ANALIZA SYGNAŁÓW GEORADAROWYCH ZAREJESTROWANYCH PODCZAS BADANIA STREF ROZLUŹNIEŃ W PŁYTKIEJ CZĘŚCI GÓROTWORU

Abstrakt

W artykule przedstawiono i omówiono niestandardowe metody przetwarzania sygnałówi obrazów georadarowych GPR (Ground Penetrating Radar) dla różnych orientacji anten pomiarowych. Badania terenowe przeprowadzono na wybranym obszarze pogórniczym w Polsce, gdzie zaobserwowano na powierzchni terenu liczne zapadliska i strefy osiadań wywołane dawną działalnością górniczą. Badania GPR przeprowadzono pomiędzy dwoma istniejącymi zapadliskami. Celem pomiarów było wykrycie stref rozluźnień w gruncie powstałych w wyniku procesów sufozyjnych, który wcześniej spowodował powstanie wspomnianych dwóch zapadlisk. W artykule zaproponowano nowy sposób przetwarzania i analizy radarogramów oparty na trzech etapach, tj. bardziej zaawansowane przetwarzanie 1D sygnałów/tras, bardziej zaawansowane przetwarzanie 2D obrazu powstałego z połączenia radarogramów i finalnie wizualizację oraz analizę wybranych atrybutów sygnałów georadarowych.

Słowa kluczowe: GPR, atrybuty sygnałów, zmienna orientacja anten pomiarowych, sufozja, rejon pogórniczy

1. INTRODUCTION

The Upper Silesia Region (Fig. 1A) is the main mining region in Poland where exploitation is conducted in numerous underground coal mines. Over mining excavations, fractured zones (in rocks) and loose zones (in grounds) are generated by mining activity and suffosion process usually extending free spaces in the geological media. Slow movement of free spaces towards the earth surface causes the appearance of sinkholes and subsidence areas which threaten the underground and overground infrastructure.

In the paper, the selected results of surveys carried out with the use of the GPR (Ground Penetrating Radar)

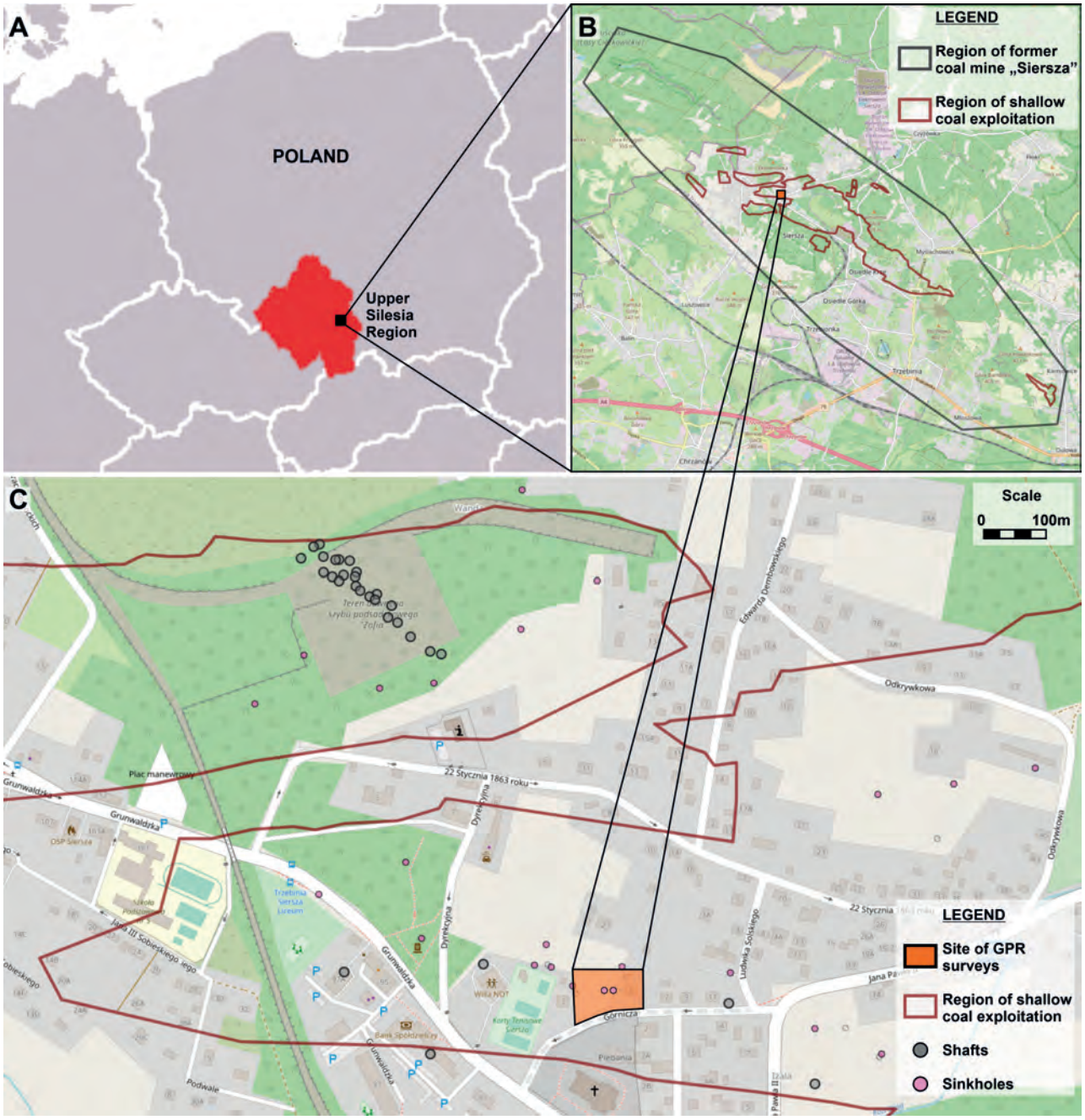

Fig. 1. A) Location of surveys site in Southern part of Poland in the Upper Silesia Region; B) location of surveys site in area of former coal mine named “Siersza”; C) detailed location of surveys site in the town of Siersza (base maps: https://zapadliska.gig.eu)

Ryc. 1. A) Lokalizacja terenu badań na obszarze Górnego Śląska (południowa Polska); B) lokalizacja terenu badań na obszarze dawnej kopalni KWK „Siersza”; C) szczegółowa lokalizacja terenu badań w miejscowości Siersza (mapa: https://zapadliska.gig.eu)

method, which is one of geophysical, electromagnetic methods, were presented. The GPR terrain measurements were conducted in the post-mining area of former coal mine named "Siersza" (Fig. 1B) in the selected region where shallow exploitation (at the depth of c.a. 26 m) was conducted (Fig. 1C). The consequence of shallow mining activity was creation of numerous sinkholes (Fig. 1C, Fig. 2A, B). Geophysical (i.e. GPR, microgravimetric, geoelectrical) surveys were conducted in presented site in several measurement sessions made since the 1990s of last century to present day [1–7]. In the paper, the author focused on the analysis of GPR data recorded on the selected profile (Fig. 2C) in 2008.

Geological information from borehole G-2 (Fig. 2D) as well as information from sinkholes (Fig. 2A, B) shows, that under the soil layer of thickness 0.5÷2.0m, few-metres-thick layer made of clayey sand occurs. Such information allows us to assume that geological settings in surveys site, to the depth of c.a. 8m are simple and sinkholes created in the loose zones of clayey sand.

At present, the GPR surveys are usually conducted in the standard way, i.e. with one orientation of transmitter and receiver antennae, which, for some situations, may cause the interpretation of results difficult and ambiguous. The standard result of GPR survey is radargram, i.e., 2D (in plane surface profile – time/depth) recording of amplitudes of electromagnetic signals reflected from underground objects, e.g. from loose and fractured zones. Detailed description of the GPR method and construction of radargram will be presented in further part of the article.

In the paper, the Author proposed to carry out non-standard terrain measurements with the application of various antennae orientations and, consequently, different electromagnetic wave polarisations. The digital GPR data recorded in such a way should be processed with the application of more advanced processing procedures and visualised in a special way in the form of signal attributes (Fig. 3).

In seismic and GPR methods, different signal attributes are often applied for different purposes. The seismic attributes were introduced as a part of the seismic interpretation in early 1970s, but much later they were used in the interpretation of GPR data. The seismic attributes are classified basically into two categories, i.e.: physical attributes and geometric attributes and they are usually used as interpretation tool for reservoir characterization [8].

In the further part of the paper, the Author focused only on selected seismic attributes, which are applied with success for years in interpretation of the GPR data, i.e. instantaneous attributes (Fig. 3), which are included into physical seismic attributes. In geophysics, electromagnetic and seismic signals are transformed from standard amplitude-time domain into others forms/domains with the use of different transforms. In the paper the Hilbert transform was applied for transformation of GPR signals into instantaneous attributes (Fig. 3).

2. FUNDAMENTS OF GPR METHOD

In the GPR method there are many different measurement techniques [6, 9, 10] i.e., short-offset reflection profiling, wide-offset reflection profiling, refraction survey, surveys with various antennae orientations and different electromagnetic wave polarisations, surveys with using of the direct ground wave, velocity measurements with mode of the WARR (Wide Angle Reflection and Refraction) and the CMP (Common MidPoint surveys) as well as tomography. At present, the most popular technique is short-offset reflection profiling (SORP) technique and it is described in the further part of the section.

In the SORP technique the transmitter (Tx) and receiver (Rx) antennae move along the profile with constant and short offset between Tx and Rx (Fig. 4). The transmitter antenna emits electromagnetic (EM) signal at every specified distance interval (Δx) and in consequence four different kinds of EM waves (which propagate in the form of a transient electromagnetic wave TEM – Fig. 5A) are created in the geological medium (Fig. 4), i.e., incident wave (IW), reflected wave (RW), transmitted wave (TW) and direct ground wave (DGW); in the air, additional direct air wave (DAW) is created but this wave does not deliver information about geological medium. In the paper, only IW and RW waves will be analysed.

Propagation of TEM wave depends on electromagnetic properties of geological medium, described by the following parameters: electrical permittivity ε [F/m], magnetic permittivity μ [H/m] and electrical conductivity σ [S/m]. For GPR method value of μ is assumed like for the vacuum and it is omitted in further analysis. Value of ε decides of the reflection of the wave and value of σ decides of attenuation of the wave; both parameters will be analysed in this section.

The TEM wave travelling through the ground (Fig. 4) loses a part of energy due to attenuation, where attenuation

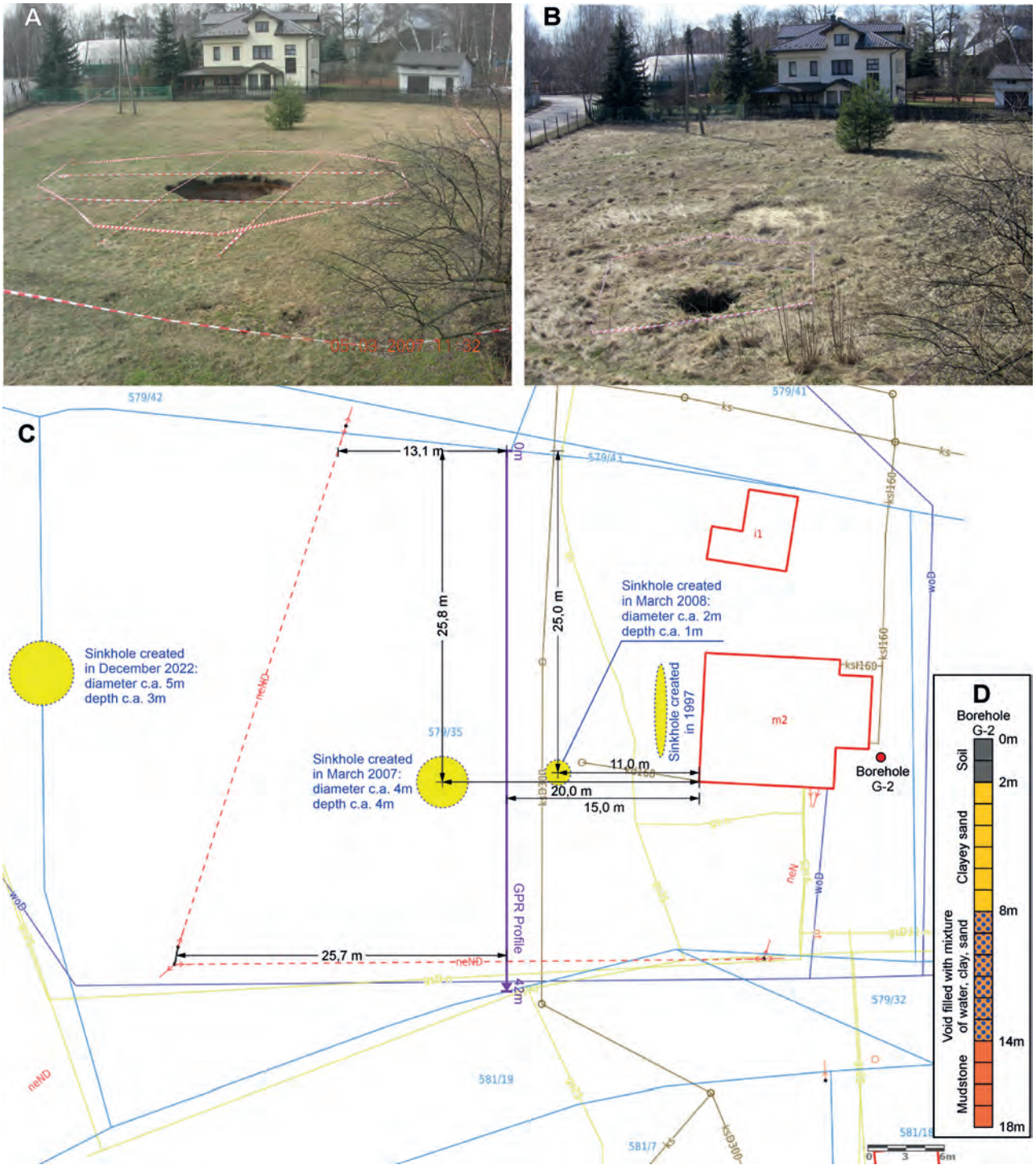

Fig. 2. Sinkholes created in GPR surveys site in 2007 (A) and 2008 (B); C) detailed positions of sinkholes and GPR profile (photos taken by Author; base map: www.geoportal.gov.pl); D) geological information from borehole G-2

Ryc. 2. Zapadliska powstałe na terenie badań georadarowych w 2007 (A) i 2008 (B); C) szczegółowa lokalizacja zapadlisk i projekt profilu pomiarowego (zdjęcie autora; mapa: www.geoportal.gov.pl); D) informacje geologiczne z otworu G-2

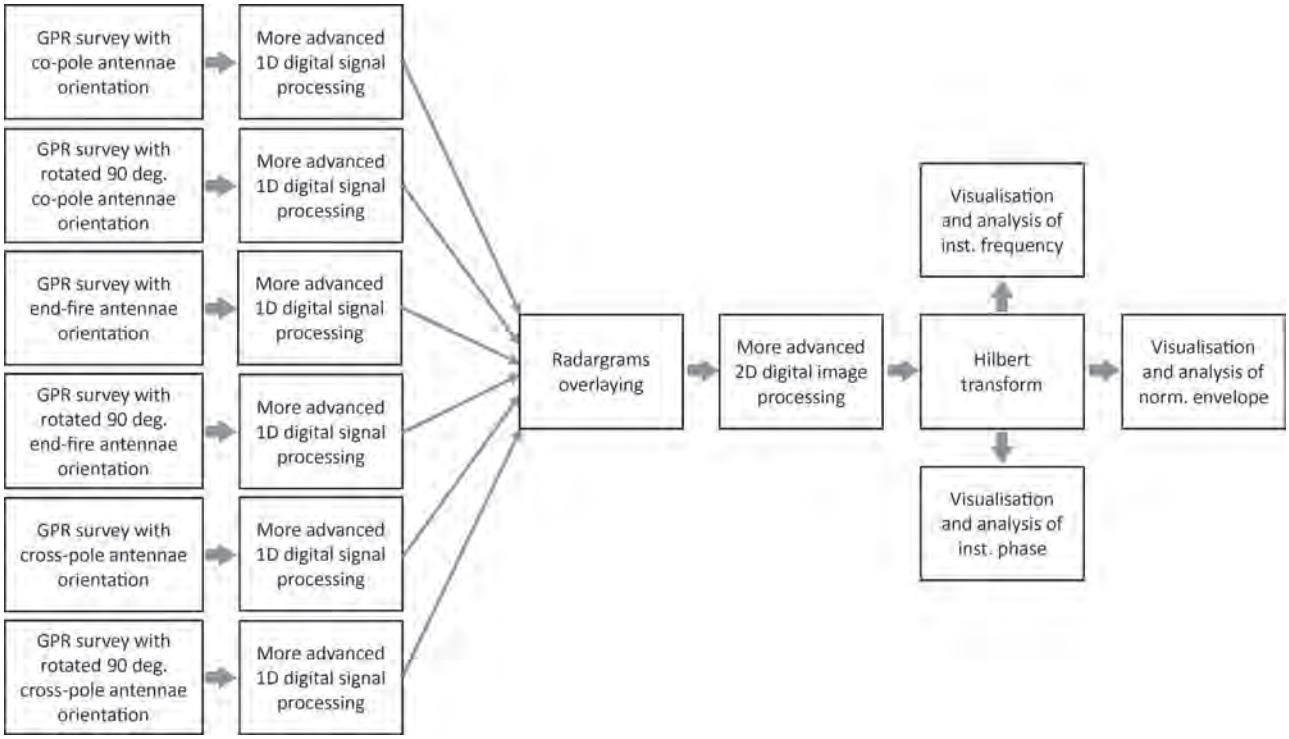

Fig. 3. Workflow of GPR data processing and visualisation
Ryc. 3. Schemat przetwarzania i wizualizacji danych georadarowych

factor α_{total} [dB/m] is defined by two components: ohmic attenuation α_o and scattering attenuation α_s according the formulae (1, 2, 3).

A part of energy of IW is reflected from underground objects and geological boundaries and propagates back to the surface as a RW and the remaining part of energy is transmitted to a deeper part of geological medium as a TW (Fig. 4).

$$\alpha_{total} = \alpha_o + \alpha_s \tag{1}$$

$$\alpha_o = 2\pi f \sqrt{\left(\frac{\varepsilon\mu}{2}\right)\cdot\left(\sqrt{1+\left(\frac{\sigma}{2\pi f\varepsilon}\right)^2}-1\right)} \tag{2}$$

$$\alpha_s = \frac{N\xi A_e}{2} \tag{3}$$

where:
f [Hz] – frequency of TEM wave;
N – number of scatterers per 1m^3;
ξ [W] – fraction of energy which is reemitted by everyone scatterers;
A_e [m^2] – effective cross section of everyone scatterers.

The contrast of values of ε in the examined medium (Fig. 4) decides upon the value of the reflection coefficient, and, in consequence, upon the amplitude of the reflections recorded on the radargram. The reflection R [-] and transmission T [-] coefficients may be calculated from formulae (4, 5, 6, 7) adequately to polarization of TEM wave (Fig. 5B, C, D).

$$R_{TE} = \frac{Z_2\cos\theta_2 - Z_1\cos\theta_1}{Z_2\cos\theta_2 + Z_1\cos\theta_1} \tag{4}$$

$$R_{TM} = \frac{Z_2\cos\theta_1 - Z_1\cos\theta_2}{Z_2\cos\theta_1 + Z_1\cos\theta_2} \tag{5}$$

$$T_{TE} = \frac{2Z_2\cos\theta_1}{Z_1\cos\theta_1 + Z_2\cos\theta_2} \tag{6}$$

$$T_{TM} = \frac{2Z_2\cos\theta_1}{Z_2\cos\theta_1 + Z_1\cos\theta_2} \tag{7}$$

where: TE refers to transverse electric component of the TEM wave and TM refers to transverse magnetic component of the TEM wave.

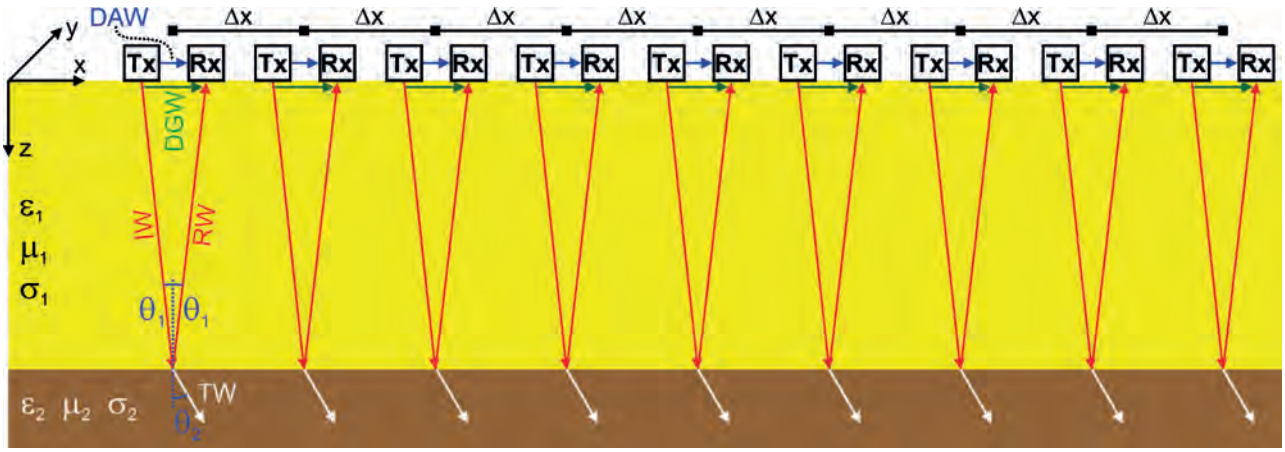

Fig. 4. Idea of the SORP survey
Ryc. 4. Idea krótko-offsetowego profilowania refleksyjnego

Value Z in formulae (4, 5, 6, 7) is a complex impedance, which describes both kinds of impedances i.e. specific Z_s and wave Z_w impedances (8, 9); for TEM wave: $Z_s=Z_w$.

$$Z_s = \sqrt{\frac{i2\pi f \mu}{\sigma + i2\pi f \varepsilon}} \qquad Z_w = \frac{\mathbf{E}}{\mathbf{H}} \tag{8,9}$$

where:
i – imaginary unit;
E [V/m] – vector of TE component of TEM wave;
H [A/m] – vector of TM component of TEM wave.

The reflected waves (RW) are recorded by the receiver antenna (Rx) and displayed on the computer during the measurements, in the form called radargram. The horizontal axis on the radargram is presented as a distance scale x [m], whereas the vertical axis is presented as a time scale t [ns]; during the processing of measured data, the time axis is converted into the depth axis z [m], taking into consideration the information about the velocity v [m/ns] of the TEM wave within the studied medium.

The standard terrain measurements are conducted with only one orientation of antennae called "co-pole" orientation (Fig. 6A). To enhance detection possibilities of GPR method as well as to make the interpretation easier and unequivocal, various antennae orientations should be applied (Fig. 6), allowing us to generate and record TEM wave with different polarizations.

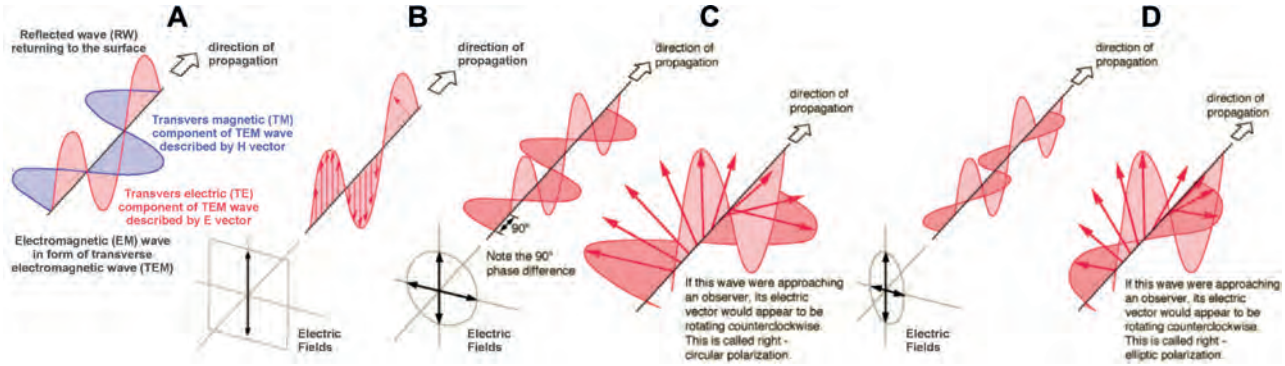

Fig. 5. A) Concept of the transient electromagnetic wave TEM; Different polarisations of the TEM wave: B) linear, C) circular, D) elliptic (www.hyperphysics.phy-astr.gsu.edu)
Ryc. 5. A) Idea poprzecznej fali elektromagnetycznej TEM; różne polaryzacje fali TEM: B) liniowa, B) kołowa, D) eliptyczna (www.hyperphysics.phy-astr.gsu.edu)

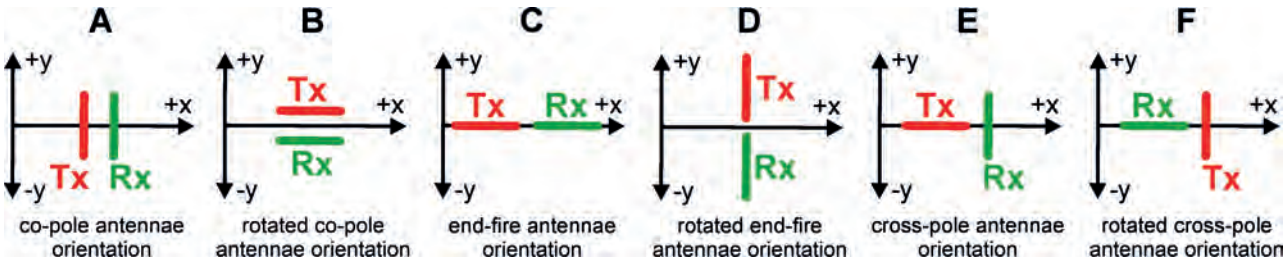

Fig. 6. Various orientations of GPR dipole antennae
Ryc. 6. Różne orientacje dipolowego układu antenowego w metodzie GPR

Due to limitation of the paper, the author does not present a theoretical background of polarisation of TEM wave in geological media but readers interested in this problem may find adequate information in [11–15].

As a general rule, the antennae orientation and, in consequence, TEM wave polarisation should be adequately adjusted to the heterogeneity and anisotropy of the geological medium as well as to the spatial distribution and geometry of any suspected underground objects. Fractured and loose zones generated by mining activity and developed by suffosion process have random distribution and there is no possibility to adjust properly antennae orientation to their distribution. Since fractured and loose zones in geological media have random distribution, it can be challenging to adjust the antennae orientation to detect them accurately. Therefore, it is advisable to use different antennae orientations during GPR terrain measurements to obtain the best possible results. Later, during the analysis of the radargrams, the interpretation can be made based either on the visual analysis of amplitude distribution in selected radargrams or (which is recommended by the Author) the methodology proposed in the paper may be applied.

3. THE RESULTS OF GPR SURVEYS

The GPR terrain measurements with application of the SORP technique were carried out along the same profile (Fig. 2C), six times with the application of various antennae orientations (Fig. 6). The GPR system produced by a Swedish firm MALA GeoScience (www.guidelinegeo.com) was used for data acquisition. The GPR surveys were conducted with 200 MHz antennae (mean resolution c.a. 0.1 m; max. depth range c.a. 10 m); traces were recorded every 0.05 m; stacking of 32 times was set during data acquisition to improve signal/noise ration.

The ReflexW computer program (www.sandmeier-geo.de) was used for processing of the GPR data and their visualization and interpretation. In the processing stage, the more advanced 1D procedures were used, i.e.: phase correction, DC shift, dewow, background removal, median filter, amplitude clipping, time-dependent Butterworth filter, spectral whitening, static correction, gain function. Detailed description of applied processing procedures may be found in [6, 9, 16–18].

For time-depth conversion, mean velocity equal 0.1 m/ns was assumed which is typical velocity for Quaternary deposits occur in the surveys site to the depth of few meters (Fig. 2D). All radargrams were presented in normalised scale with normalisation of signals amplitudes to max. amplitude of the DAW.

In Fig. 7A radargram for "co-pole" antennae orientation and in Fig. 7B for "rotated of 90 deg. co-pole" orientation were presented.

Main anomalous zone in both radargrams may be distinguish between x=18÷42 m and z=0÷3 m; it was interpreted as a loose part of clayey sand where increasing of porosity was caused initially by shallow mining activity and then by suffosion process. Direction of inflow of underground water is observed from the end part of the profile. For both orientations of antennae, the radargrams are similar, but in Fig. 7B additional, linear anomaly is observed; it might be assumed that this anomaly was caused by electrical cable located near the profile at distances 13.1 m and 25.7 m (Fig. 2C); however, putting into the computer program velocity 0.3 m/ns (which is typical for the air) such anomaly would be observed in the radargram if electrical cable occurred in distance 9.5 m and 14.5 m (Fig. 7B); finally it was assumed that this anomaly origins from the underground boundary, and standard antennae orientation (Fig. 7A) did not reveal such geological boundary.

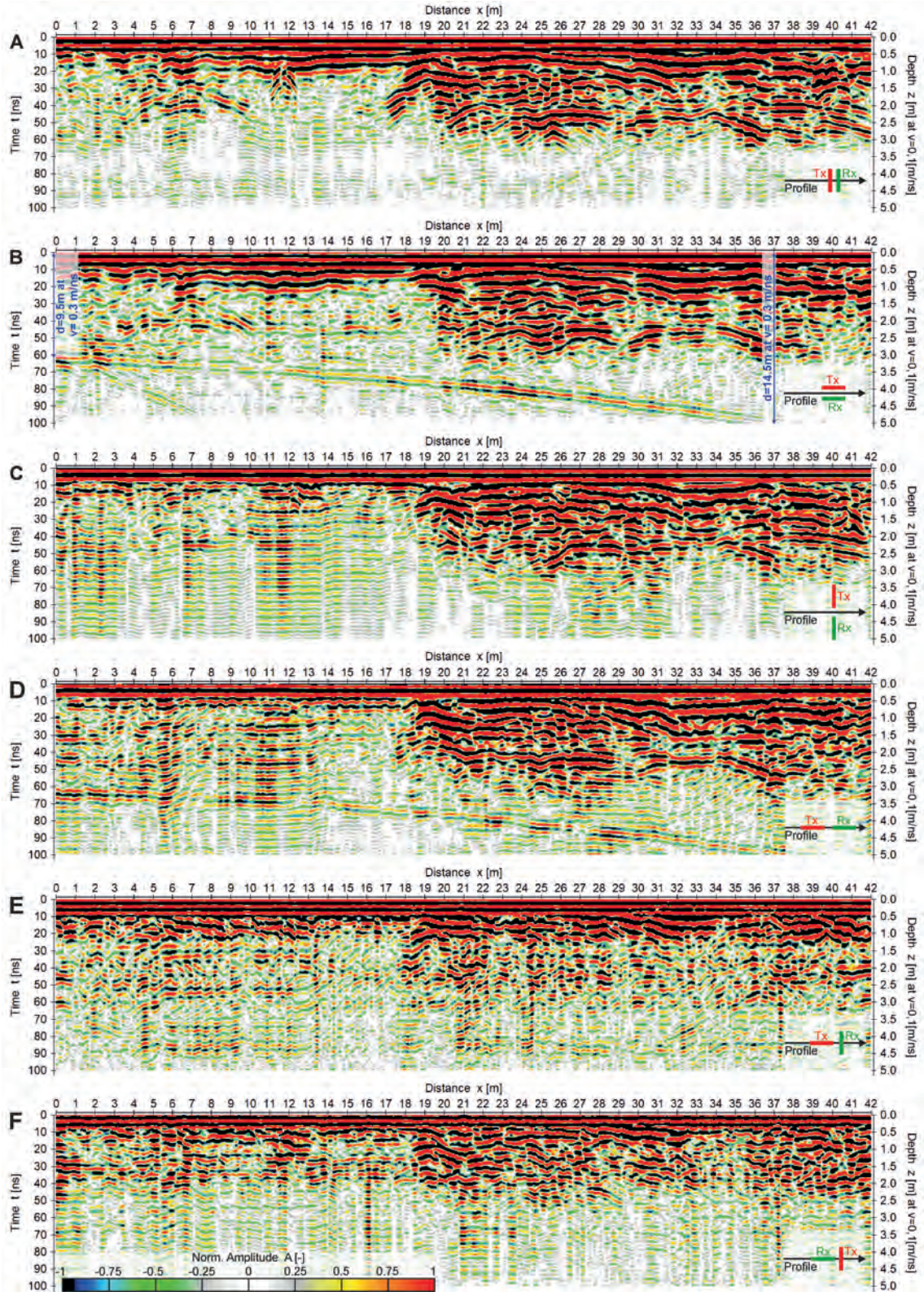

Fig. 7. Radargrams after more advanced 1D processing for various antennae orientations
Ryc. 7. Radargramy po zastosowaniu bardziej zaawansowanego przetwarzania 1D dla różnych orientacji anten

In Fig. 7C radargram for "end-fire" antennae orientation and in Fig. 7D for "rotated of 90 deg. end-fire" orientation were presented. Both radargrams deliver the same information about location of main anomalous zone like in Fig. 7A, B. For "rotated of 90 deg. end-fire" orientation (Fig. 7D) the same linear anomaly was recorded like for "rotated of 90 deg. co-pole" orientation (Fig. 7B); it seems that such antennae orientations are more sensitive for detection of underground objects/boundary occuring in the survey site.

The worst information concerning distribution of loose zones was delivered by "cross-pole" and "rotated of 90 deg. cross-pole" antennae orientations (Fig. 7E, F).

In the next stage of data processing and analysis, information from all radargrams were overlayed and such combined radargram was subjected to 2D digital image processing (Fig. 3).

4. THE RESULTS OF GPR SIGNALS ATTRIBUTES ANALYSIS

Radargram has a specific feature, i.e. it is a collection of signals/traces (Fig. 8A) which may be treated as a digital image (Fig. 8C). Therefore, every trace was processed independently with the application of 1D processing procedures but digital form of signals/traces

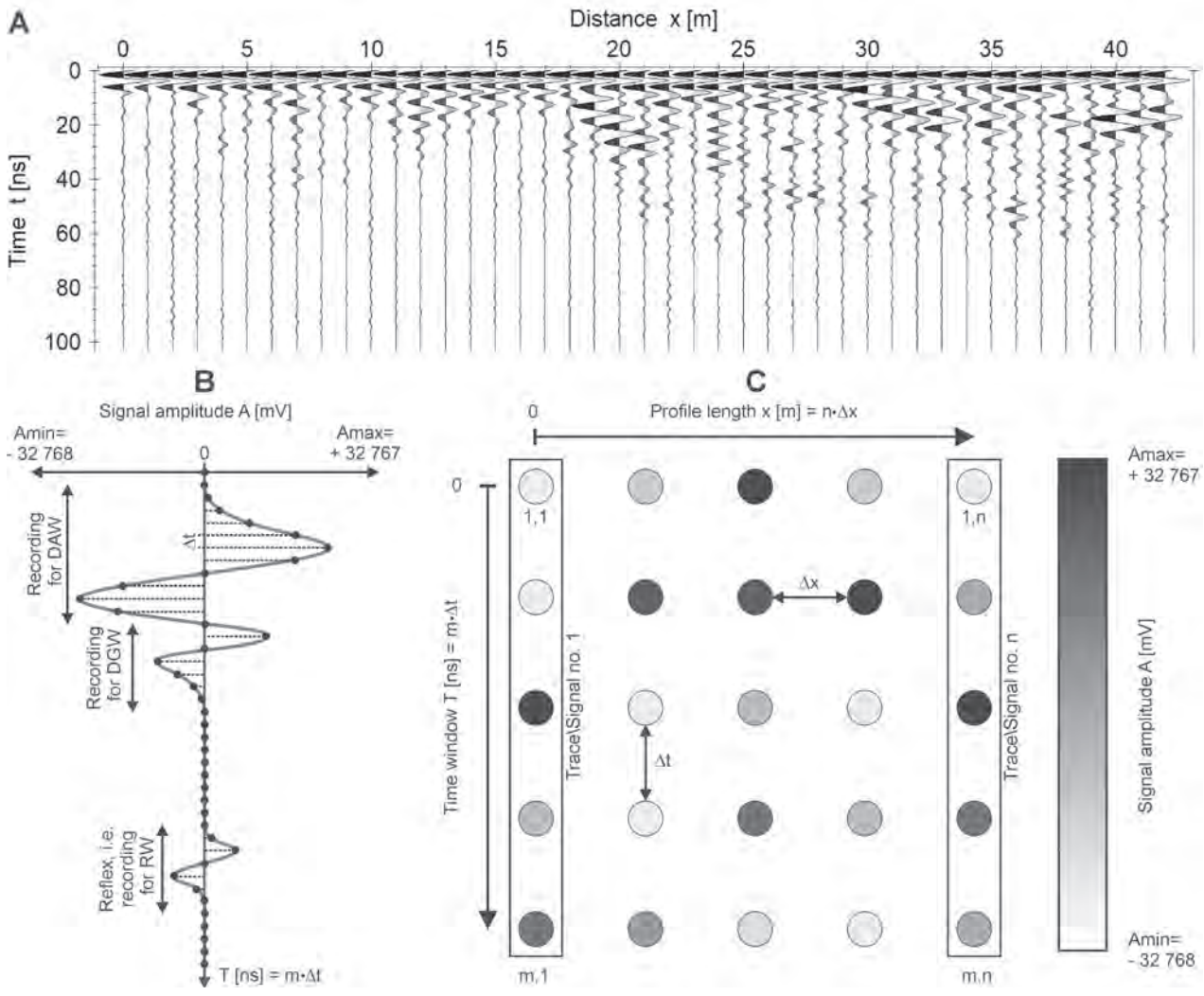

Fig. 8. Example presentation of signals/traces recorded for "co-pole" antennae orientation – for better visualisation only every 20th signal/trace was shown; B) Construction of digital signal/trace; C) Presentation of signals in the form of digital image
Ryc. 8. Przykład sygnałów/tras zarejestrowanych dla orientacji anten typu „co-pole" – dla lepszej wizualizacji pokazano tylko co dwudziestą trasę/sygnał; B) konstrukcja cyfrowego sygnału/trasy; C) prezentacja sygnałów w formie obrazu cyfrowego

(Fig. 8B) allowed to convert collection of traces into digital image and application of 2D image processing procedures was possible.

After the application of 1D processing on every radargram (Fig. 7) one combined radargram constructed by overlaying of several radargrams (Fig. 7) was created (Fig. 9A). Combined radargram was subjected to 2D image processing, in three steps; at first applied: x-z interpolation, stacking, Stolt migration, median filtering (Fig. 9A); afterwards, for image from Fig. 9A, instantaneous attributes, i.e. instantaneous amplitude, instantaneous frequency and instantaneous phase, was calculated from Hilbert transform; in the third step, morphologic filtration, i.e. erosion and dilatation, was applied (Fig. 9B, C, D). Detailed description of the applied processing procedures can be found in [2, 6, 9, 15–18]. The Hilbert transform will be described in more detail, as the results of this transform were analysed.

The GPR signal/trace may be treated as a polyharmonic function of amplitude vs time A(t) – Fig. 8B. Such signal may be described as a complex trace Ψ(t) in the following form [17]:

$$\Psi(t) = A(t) + i \cdot B(t) \tag{10}$$

where:

A(t) – real part of Ψ(t) which is a recorded signal;

B(t) – imaginary part of Ψ(t) which is Hilbert transform of signal where phase angle of all components of signal are shifted by ±90 deg.

From complex trace Ψ(t), the instantaneous amplitude E(t) may be calculated (11).

$$E(t) = \sqrt{|\, Re\Psi(t)\,|^2 + |\, Im\Psi(t)\,|^2} \tag{11}$$

The instantaneous amplitude, called also a signal envelope, is a measure of the intensity of the reflection coefficients, proportional to the square root of the total signal energy at a given moment of time; the envelope may be treated as a measure of the signal energy.

Other signal attribute which can be calculated from the complex trace is the instantaneous phase (12), which is a measure of the continuity of anomalies in the radargram.

$$\varphi(t) = arctg\left(\frac{Im\Psi(t)}{Re\Psi(t)}\right) \tag{12}$$

And the third signal attribute calculated from the complex trace is the instantaneous frequency (13) which determines the rate of change of the instantaneous phase.

$$f(t) = \frac{d\varphi(t)}{dt} \tag{13}$$

In Fig. 9A a combined radargram in normalised form was presented. Main anomalous zone which depicts a huge loose zone of ground is easily noticed. As it was mentioned during the interpretation of Fig. 7, loose zone was created by suffusion process and, in consequence both sinkholes (Fig. 2A, B) were created.

In Fig. 9B the instantaneous amplitudes (i.e. signals envelope) in normalised form are shown; for more detailed separation of anomalies, values between 0.8 and 1.0 were divided into sub-anomalies by isolines with step 0.04 (Fig. 9B – white isolines). Visualisation of anomalies in the form of an envelope allows more detail description of regions with high porosity in which water flows in the ground and suffosion process is the most intensive. It should be mentioned that surveys were conducted after creation of both sinkholes, so anomalies indicate the new dangerous regions of ground between sinkholes.

As it was mentioned above, the instantaneous phase (Fig. 9C) may be treated as an indicator of continuity of anomalies in the radargram. Seven characteristic regions with linear continuity of anomalies were outlined in Fig. 9C. All these regions (beside Anomaly 6) are located outside of main anomalies depicted in Fig. 9A, B therefore there is no possibility to correlate them. The attempt of correlation of Anomaly 6 (Fig. 9C) with anomalies in Fig. 9A, B delivered no valuable results because loose zones have random, not linear, distribution in the ground.

In Fig. 9D the instantaneous frequency was presented and main anomalies from Fig. 9A, B, C were inserted into this figure. As it was mentioned, the instantaneous frequency determines the rate of change of the instantaneous phase. In Fig. 9D there is no possibility in unequivocal way to correlate information between the instantaneous frequency, the instantaneous phase and the instantaneous amplitudes (envelope). Most likely, this results from the fact that loose zones have random distribution in the geological medium.

Usually, results of attribute analyses are calibrated to direct information of the underground (i.e. with

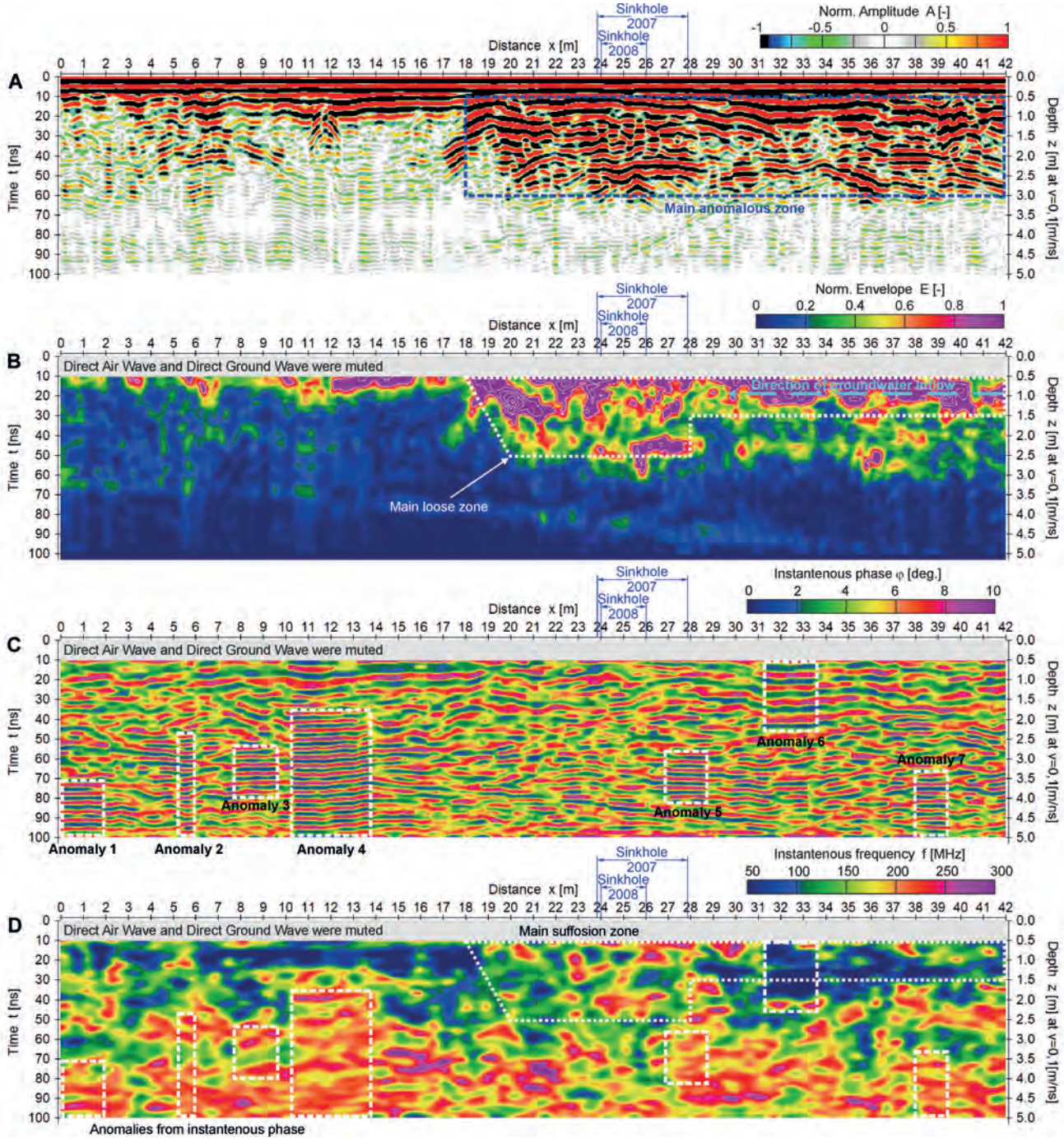

Fig. 9. A) Combined radargram after 2D processing; B) Instantaneous amplitude – envelope; C) Instantaneous phase; D) Instantaneous frequency

Ryc. 9. Wynikowy połączony radargram po przeprowadzeniu przetwarzania 2D; B) amplituda chwilowa; C) faza chwilowa; D) częstotliwość chwilowa

Fig. 10. A) Injection of filling material to the lose zones in 2013 (www.google.com/maps – street view); B) the sinkhole appearing in the survey site in December 2022 (https://wiadomosci.onet.pl/krakow/) – detail location is shown in Fig. 2C
Ryc. 10. Iniekcja materiału wypełniającego do stref rozluźnień w 2013 (www.google.com/maps – street view); B) zapadlisko powstałe w miejscu badań georadarowych w grudniu 2022 (https://wiadomosci.onet.pl/krakow/) – dokładną lokalizację pokazano na ryc. 2C

borehole information) at some calibration points in order to justify the interpretation of the results at other places without direct information. The GPR surveys were conducted in distance of a few meters from both sinkholes (Fig. 2C), so the appearance of anomalies in attribute distributions may be directly correlated with the presence of loose zones, which caused the formation of both sinkholes. The analysis of GPR signal envelope was also carried out for region around borehole G-2 [6] and similar anomalies like those interpreted in Fig. 9B were observed in radargram below depth of 8m, in loose zone filled with water, clay and sand (Fig. 2D). Few years after the GPR surveys, in 2013, filling material was injected into the ground (Fig. 10A) and colmatation of geological medium was observed mainly in near surface underground where many loose zones occurred. Presence of loose zones in shallow depths, in clayey sand, was confirmed by the appearance of the next sinkhole, in 2022 (Fig. 10B).

5. CONCLUSIONS

The GPR surveys carried out for various antennae orientations and, in consequence, for different polarisations of electromagnetic wave delivered more information about loose zones distribution than standard GPR measurements. Application of more advanced processing procedures and construction of combined radargram allowed to present the main anomalous zone in unequivocal form. Visualisation of anomalies in the form of the instantaneous amplitudes (envelope) distribution allowed more detail outline of loose zones created by the suffosion process. It seems that other signal attributes i.e. the instantaneous phase and frequency are not useful for interpretation due to the fact that the loose zones in the ground have a random distribution.

REFERENCES

1. Ziętek, J.; Karczewski, J.; Tomecka-Suchoń, S.; Carcione, J.; Padano, G.; Denis, C. Observations and Results of GPR Modelling of Sinkholes in Upper Silesia (Poland). Acta Geodetica and Geophysica Hungarica, vol. 36(4), 2001, pp. 377–389.
2. Marcak H.; Gołębiowski, T. Analysis of GPR Trace Attributes and Spectra for LNAPL Contaminated Ground. Proceedings of the International Conference "Near Surface 2006", EAEG Org., Helsinki, Finland, paper no. P020, 2006.
3. Marcak, H.; Gołębiowski, T.; Tomecka-Suchoń, S. Spatial-Time Analysis of Georadar Data for the Risk Assessment of Post-Mining Voids. Proceedings of the Polish Conference "Mining Workshops 2007" (Abstract in: WUG monthly – Occupational Safety and Environmental Protection in Mining), CPPGSMiE PAN Org., Ślesin, Poland, 2007, pp. 309––324 (in Polish).
4. Marcak, H.; Gołębiowski, T.; Tomecka-Suchoń, S. 3D GPR measurements for Sinkholes Detection – Case Studies from Selected Sites in Poland. Proceedings of the International Conference "Near Surface 2008", EAEG Org., Cracow, Poland, 2008a.

5. Marcak, H.; Gołębiowski, T.; Tomecka-Suchoń, S. Geotechnical Analysis and 4D GPR Measurements for the Assessment of the Risk of Sinkholes Occuring in Polish Mining Area. Near Surface Geophysics, vol. 6, no. 4, 2008b, pp. 233–243.
6. Gołębiowski, T. Application of the GPR Method for Detection and Monitoring of Objects with Stochastical Distribution in the Geological Medium. AGH-UST Ed., Cracow, Poland, 2012, pp. 256 (in Polish).
7. Tomecka-Suchoń, S.. Estimation of sinkhole hazard by GPR 4D method for the purpose of foundation treatments on post-mining areas. Mining Review, vol. 70, no.7, 2014, pp. 56–60 (in Polish).
8. Subrahmanyam, D.; Rao, P.H. Seismic Attributes – A Review. Proceedings of 7th International Conference and Exhibition on Petroleum Geophysics, Hyderabad, India, 2008, pp. 398.
9. Annan, A.P. Ground Penetrating Radar. Workshop Notes, Sensor and Software Inc., Canada, 2001.
10. Gołębiowski, T.; Małysa, T. The Application of Non-Standard GPR Techniques for the Examination of River Dikes. Technical Transactions, vol. 115, no. 7, 2018, pp. 121––138.
11. Roberts, R.L.; Daniels, J.J. Analysis of GPR Polarization Phenomena. Journal of Environmental and Engineering Geophysics 1(2), 1996, pp. 139–157.
12. Guy, E.D.; Daniels, J.J.; Radzevicius, S. Demonstration of Using Crossed Dipole GPR Antennae for Site Characterization. Geophysical Research Letters, 26(22), 1999, pp. 3421–3424.
13. Daniels, J.J.; Wielopolski, L.; Radzevicius, S.; Bookshar, J. 3D GPR Polarization Analysis for Imaging Complex Objects. Proceedings of the SAGEEP Int. Conference, San Antonio, USA, 2003, pp. 585–597.
14. Gołębiowski, T.; Tomecka-Suchoń, T. GPR Fractures Detection Using Changeable Antennae Orientation. Proceedings of the International Conference and Exhibition, St. Petersburg. Russia, 2012.
15. Marcak, H.; Gołębiowski, T. The Use of GPR Attributes to Map a Weak Zone in a River Dike. Exploration Geophysics, 45(2), 2014, pp. 125–133.
16. Annan, A.P. Practical Processing of GPR Data. Sensor and Software Inc., Canada, 1999.
17. Yilmaz, O. Seismic Data Processing. Society of Exploration Geophysicists, Tulsa, USA, 1994.
18. Kasina, Z. Seismic Processing. CPPGSMiE PAN Ed., Cracow, Poland, 1998, pp. 333 (in Polish).